

# The Synthesis and Assembly of Polymeric Microparticles Using Microfluidics

By *Dhananjay Dendukuri*, and *Patrick S. Doyle\**

The controlled synthesis of micrometer-sized polymeric particles bearing features such as nonspherical shapes and spatially segregated chemical properties is becoming increasingly important. Such particles can enable fundamental studies on self-assembly and suspension rheology, as well as be used in applications ranging from medical diagnostics to photonic devices. Microfluidics has recently emerged as a very promising route to the synthesis of such polymeric particles, providing fine control over particle shape, size, chemical anisotropy, porosity, and core/shell structure. This progress report summarizes microfluidic approaches to particle synthesis using both droplet- and flow-lithography-based methods, as well as particle assembly in microfluidic devices. The particles formed are classified according to their morphology, chemical anisotropy, and internal structure, and relevant examples are provided to illustrate each of these approaches. Emerging applications of the complex particles formed using these techniques and the outlook for such processes are discussed.

## 1. Introduction

The use of polymeric particles can be traced back to the ancient Mayans who used natural rubber – a suspension of polymeric microparticles – for a variety of applications. In the past century polymer science witnessed an explosive growth, resulting in the discovery and development of a number of new synthetic polymers. Dispersions of particles made from several of these polymers are now commonly used to provide effective protection, binding and finishing to a number of industrial products such as paper, metals and wood.<sup>[1]</sup> Gradually, polymeric particles have also found use in high value biological and analytical applications including as column supports for chromatography, beads for flow cytometry and in the recovery of DNA and proteins. The use of polymeric particles has spread from applications requiring bulk quantities of particles to niche applications in photonics, diagnostics and tissue engineering where the properties of each individual particle are critical to their technological function. With this, the requirements on particle monodispersity,

chemistry, porosity, shape and size are becoming increasingly stringent.

Currently, the most common approach to the synthesis of dispersions of polymeric particles at the colloidal length scale is emulsion polymerization. In a typical industrial reactor, a monomer is emulsified in an aqueous solution containing a suitable surfactant and an initiator molecule. Upon heating this mixture, particles are first nucleated from surfactant micelles and then continue to grow in size until the desired diameter is reached. The reaction is terminated at an appropriate time to obtain particles of a desired size across the colloidal length scale; up to a few micrometers. The predominant shape obtained is a sphere. Although spherical shapes are sufficient and indeed desirable for many applications, there has been a growing realization of the necessity for custom-designed, nonspherical particles for several applications.

For instance, particle-based assays are expected to compete with and even replace standard substrate-based assays such as enzyme-linked immunosorbent assays (ELISAs) in the future.<sup>[2]</sup> This is due to their ability to perform multiple protein measurements using a single sample while at the same time reducing sample volume requirements. In such applications, tight monodispersity standards and the ability to provide for multiplexing by encoding a unique identity into each particle are essential to provide accurate measurements. A number of recent studies have also explored the use of particles as building blocks for the synthesis of complex structures. One promising application for polymeric particles here is to use them to build photonic crystals through the assembly of individual particles.<sup>[3]</sup> These crystals possess the ability to selectively filter out certain wavelengths of light. In such applications, anisotropic particles that exhibit preferential self-assembly in one direction expand the range of crystal structures formed and are essential to providing finely tunable photonic band gaps. Further, there is a requirement for the development of techniques to controllably assemble such particles into organized superstructures. In the bottom-up approach envisioned to build the materials and devices of the future, precisely shaped and patterned ‘patchy’ particles will be essential to function as encoded building blocks that self-assemble into the required superstructure.<sup>[4]</sup> There is also a need for spherical monodisperse polymeric particles in the range of several micrometers and above for chromatography and liquid

[\*] Prof. P. S. Doyle, Dr. D. Dendukuri  
66-270, 77 Massachusetts Avenue  
Department of Chemical Engineering  
MIT, Cambridge MA 02139 (USA)  
E-mail: pdoyle@mit.edu

DOI: 10.1002/adma.200803386

crystal spacer applications. The synthesis of such particles using existing techniques like seed polymerization is time consuming and expensive. Polymeric particles also find wide use as carriers for drug molecules. Recently, particle shape was shown to be an important parameter that regulated the performance of drug carrier.<sup>[5]</sup>

To address the needs in these different areas, several innovative processes for the synthesis of polymeric particles have been recently developed. These include template-based printing,<sup>[6]</sup> mold stretching,<sup>[7]</sup> photolithographic fabrication,<sup>[8]</sup> and several microfluidics-based processes. While each of these processes has its own advantages, in this report we will focus on microfluidics-based processes. Although several methods to synthesize nanoparticles inside microfluidic devices have also been developed,<sup>[9–13]</sup> this article will focus on the synthesis and assembly of micrometer-scale polymeric microparticles. Several insightful reviews<sup>[14–16]</sup> covering different aspects of microfluidic particle synthesis have been published in the past few years and have focused mainly on droplet formation<sup>[17]</sup> as the basis for particle synthesis. Other techniques developed more recently such as flow lithography, as well as a class of techniques that utilizes particle assembly inside microfluidic devices provide an even wider range of particle morphologies and potential applications that have not been covered in great detail. Also, with the emphasis shifting away from merely describing fabrication techniques, there is a need to critically examine the potential applications of particles synthesized using these methods.

While the field of microfluidics has largely been devoted to developing miniaturized analytical tests for biological and chemical applications, several synthesis applications have also been reported in recent years. The ability to provide controlled environmental conditions, continuous flow systems and laminar flow at the microfluidic length scale have all contributed to the growth of microfluidics for such applications. Among these, a prominent application has been the controlled synthesis of micrometer-sized polymeric particles inside microfluidic devices. Polymeric particle synthesis using microfluidics can be broadly classified into three different methods:

- 1) Droplet-based and multiphase flow methods
- 2) Photolithography based methods
- 3) Supraparticle synthesis using assembly of colloids

The degree of chemical anisotropy, shape complexity, and size that can be attained using current processes including microfluidic ones is summarized in Figure 1.

## 2. Droplet-Based Particle Synthesis

The ability to create monodisperse emulsions inside microfluidic devices has spawned several areas of research including the creation of monodisperse solid particles. Inspired by the concept of membrane emulsification, in 1997 the Nakajima group first demonstrated the controlled formation of micrometer-sized oil-in-water (O/W) and water-in-oil (W/O) emulsion droplets in a micromachined silicon device.<sup>[18]</sup> Sunflower-oil-in-water or water-in-oil emulsions stabilized by suitable surfactants were



**Dhananjay Dendukuri** received his Ph.D. in Chemical Engineering from MIT in 2007. Prior to this, he obtained a MASC and B.Tech in Chemical Engineering from the University of Toronto and Indian Institute of Technology-Madras respectively. He received the Senturia Prize (2007) for the best thesis work in the area of MEMS and NEMS at MIT. He is currently at Connexios Life Sciences, India

where he is developing automated microfluidic assays for drug discovery and diagnostics.



**Patrick Doyle** earned his Ph.D. in Chemical Engineering at Stanford University in 1997. After a postdoctoral fellowship at the Institute Curie in Paris, he joined the MIT Chemical Engineering faculty in 2000. He was promoted to associate professor with tenure in 2008. Prof. Doyle's research focuses on translating a molecular understanding of transport phenomena into new microfluidics-based processes.

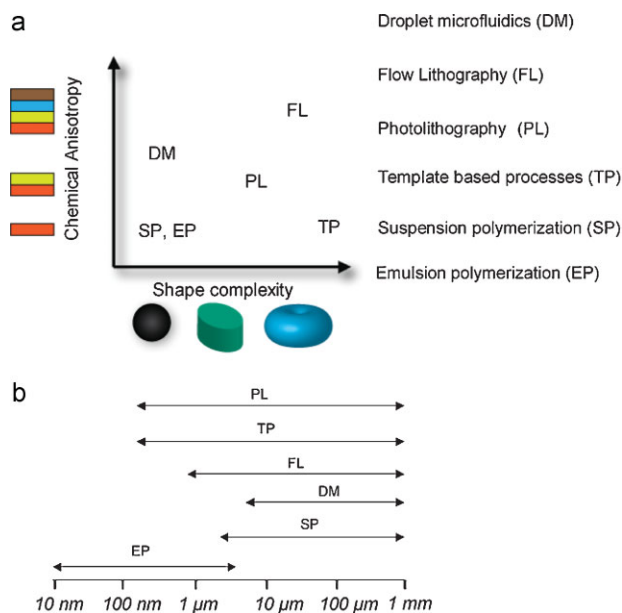


**Figure 1.** a) Different processes extant for particle synthesis classified according to their ability to synthesize complex shapes and multifunctional particles. b) Particle size range covered by the same processes.

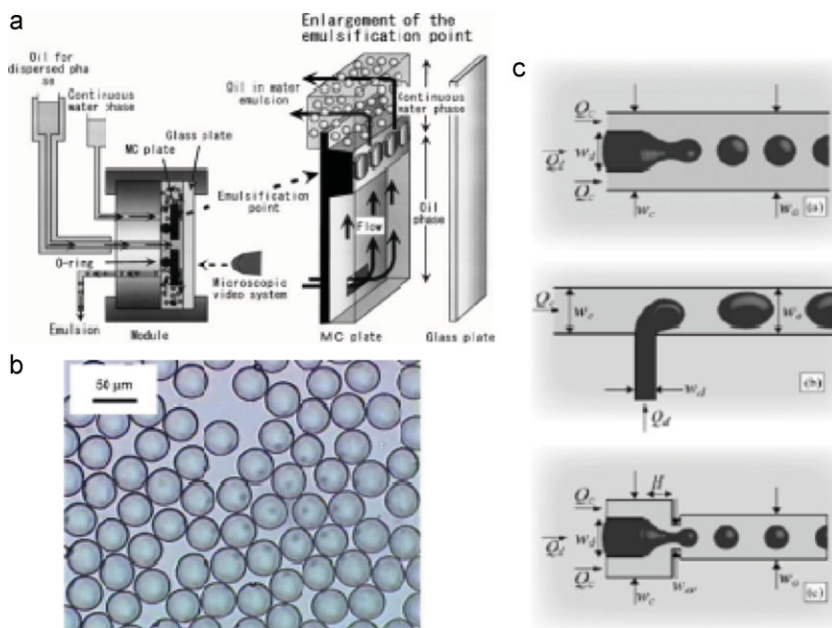


**Figure 2.** a) The first micromachined, silicon based microfluidic device used for droplet generation. Reproduced with permission from [29]. Copyright 2001 Elsevier. b) Spherical particles synthesized using a microfluidic T-junction based device. Reproduced with permission from [33]. c) Standard geometries used for controlled droplet formation in microfluidic devices – Coflow, T-junction and the Flow-focusing Device (FFD). Reproduced with permission from [17]. Copyright 2007 Institute of Physics.

obtained using the device shown in Figure 2a. A pressurized dispersed phase was forced onto a terrace through a series of micrometer-sized slits micromachined into a silicon microchannel module bonded by a glass plate. The dispersed phase was extruded into a reservoir containing a continuous phase. While entering the reservoir, droplets of the dispersed phase were broken off by surface tension effects and were subsequently viewed through the glass plate. The material of the device was chosen based on the surface properties of the liquid constituting the continuous phase. Silicon was chosen for O/W emulsions and hydrophobically modified silicon was chosen to make W/O emulsions. The size of the droplets formed ( $22.5\ \mu\text{m}$ ) was approximately three times as large as the slit widths ( $6\ \mu\text{m}$ ) in agreement with previously observed empirical relations seen during membrane emulsification. The authors also reported that the droplet size was a strong function of the slit width and depended only weakly on the pressure of the dispersed phase.

### 2.1. T-junction Based Droplet Formation

Following the work on microchannel emulsification using a membrane inspired approach, in 2001 the Quake group formed controlled emulsions using a T-junction microchannel made in polydimethylsiloxane (PDMS, Fig. 2c, middle).<sup>[19]</sup> Droplets of the dispersed phase are broken off by a combination of the shear forces exerted by the continuous phase and the squeezing effect exerted by the continuous phase when the dispersed phase fills up the continuous phase channel.<sup>[20]</sup> The advantage of this method is that droplet size is not dependent only on the channel width but

can also be controlled by changing the input pressure gradient or flow rates of the dispersed or continuous phase. A number of recent papers have explored the physics behind the droplet formation at a T-junction.<sup>[17]</sup> The important dimensionless parameters in this geometry are the ratio of the flow rates of the continuous and dispersed phase,  $Q_d/Q_c$ , and the Capillary number,  $Ca$  which is the ratio of shear forces exerted by the continuous phase to the surface forces at the interface.

$$Ca = \frac{\mu v}{D} \quad (1)$$

At low values of  $Ca$ , droplet size is solely a function of  $Q_d/Q_c$ .<sup>[20]</sup> At larger values of  $Ca$ , shear forces also come in to play, droplet size decreasing with increasing  $Ca$ . Droplet break-off using Y-junctions has also been reported.<sup>[21]</sup> Unlike T-junctions, it was found that droplet size is dependent solely on  $Ca$  and the channel depth and not on  $Q_d$ .<sup>[22]</sup>

### 2.2. Flow-Focusing Device Based Droplet Formation

A planar flow-focusing device (FFD) geometry (Fig. 2c, bottom) was first implemented in a microfluidic device to form droplets in a controlled manner by the Stone group.<sup>[23]</sup> Previous efforts at implementing a FFD geometry were made at the macroscale in order to make monodisperse bubbles.<sup>[24]</sup> In the planar FFD geometry, a coaxially flowing continuous phase fluid flanks the dispersed phase on either side leading to droplet break off soon after a narrow orifice through which both fluids are extruded. In contrast to the T-junction geometry, the FFD geometry produces flows with strong elongational kinematics, where fluid elements are primarily stretched rather than rotated.

While the T-junction geometry is relatively simple to use, permitting the regular creation of monodisperse droplets over a wide range of flow rates, the FFD device must be optimized with more attention to the geometry and flow conditions in order to yield regular sized droplets. On the other hand, the FFD geometry seems more amenable to scale-up by parallelization while parallelizing the T-junction geometry can lead to multimodal or chaotic processes where the droplet size is not uniform at every junction.<sup>[17]</sup>

### 2.3. Coflow Based Droplet Formation Devices

In addition to the crossflow (T-junction) and flow-focusing (FFD) geometries discussed, a third type of geometry that has been exploited to form droplets is the coflowing geometry (Fig. 2c, top). Here, the dispersed and continuous phases flow parallel to each other. Seong and coworkers<sup>[25]</sup> implemented this configuration



using a glass pipette inserted into a PDMS device to create a hollow channel for the continuous phase to flow through.

In addition to the planar devices synthesized, capillary devices possessing cylindrical symmetry have also been used for the implementation of droplet formation devices. Coflow,<sup>[26]</sup> crossflow,<sup>[27]</sup> and flow-focusing<sup>[28]</sup> have all been implemented in these geometries to synthesize droplets. Capillary devices possess certain advantages like fabrication using off-the-shelf components, ease of formation in FFD type of geometries due to their 3D nature and relative unimportance of surface effects leading to easier droplet formation. On the other hand, synthesizing arbitrary geometric configurations and achieving length scales less than 100  $\mu\text{m}$  is difficult.

A variety of mechanisms have been used to convert droplets formed in microfluidic devices into solid particles. The mechanisms used for particle formation can be broadly classified into 1) heat-based, 2) light-based, and 3) chemical-reaction-based methods. In heat-based methods, thermally polymerizing the droplet or simply using high melting point oils that can be cooled into solids at room temperature is the basis for particle formation. In light-based methods, external radiation such as ultraviolet light is shone on droplets comprised of photosensitive moieties in order to convert them to solid particles. Chemical reaction based methods are unique in not requiring any external impulse to achieve particle formation. In such methods, a chemical species that is essential for the polymerization is added separately to a droplet at a desired time and location to achieve polymerization. In the next sections we provide representative examples of each of these. The basic idea is the same in all cases. The discrete phase/s are comprised of a thermally, photochemically or chemically curable material that can harden upon application of the right stimulus to convert the liquid droplets into solid microparticles.

## 2.4. Spherical Particles

In the first demonstration of microsphere formation from a microfluidic device, Nakajima and coworkers synthesized solid lipid microspheres made from hydrogenated fish oil.<sup>[29]</sup> Oil-in-water droplets were first generated at a temperature of 70  $^{\circ}\text{C}$ , and then solidified and freeze-dried to yield solid microspheres in the range of 20  $\mu\text{m}$ . The coefficient of variation (CV) in size of the beads was reported to be less than 5%, a significant improvement over suspension polymerization approaches which are traditionally used for the synthesis of beads in the range of 10  $\mu\text{m}$  and above. The same authors later used thermal polymerization to form polystyrene microspheres using divinyl benzene as the starting material and benzoyl peroxide as a reaction initiator.<sup>[30]</sup> The spheres formed were in the

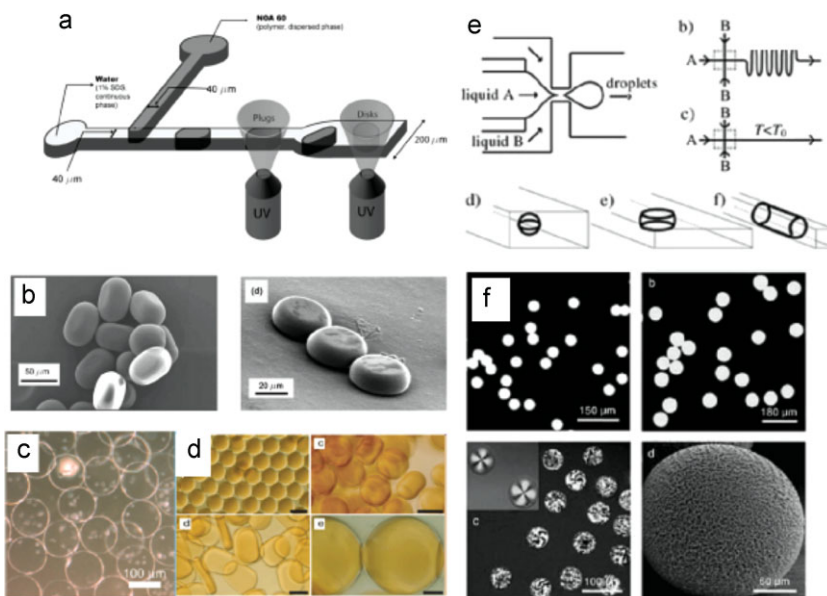


**Figure 3.** Complex, homogeneous particles synthesized using droplet-based microfluidic methods. a) Geometry used to synthesize non-spherical plug and disk shaped particles using a T-junction based approach. Reproduced with permission from [34]. Copyright 2005 American Chemical Society. b) SEM images of the particles formed from the device shown in (a). c) Cell encapsulated alginate particles synthesized using a droplet-based method. Reproduced with permission from [32]. d) Monodisperse and homogeneous magnetic particles formed using droplets at a T-junction. Reproduced with permission from [45]. Copyright 2008 Royal Society of Chemistry. e) FFD geometry used to form non-spherical particles in a variety of polymers. Reproduced with permission from [35]. f) Particles formed using the device shown in e).

range of 5–10 micrometers ( $\text{CV} \approx 5\%$ ). The synthesis of monodisperse, micrometer-sized alginate beads is very important for applications in column chromatography to ensure uniform and predictable reaction kinetics. In an example of chemical reaction mediated synthesis, Sugiura et al. formed 50–200  $\mu\text{m}$  size alginate beads by first forming droplets of alginate using a micro-nozzle that were then solidified by the addition of  $\text{CaCl}_2$ .<sup>[31]</sup> Takeuchi and coworkers formed very monodisperse alginate beads (Fig. 3c) by using an internal gelation approach where nano-sized  $\text{CaCO}_3$  particles were dispersed along with the droplet forming phase.<sup>[32]</sup> A pH change induced by acetic acid present in the oil phase was used to break down the nanoparticles and release  $\text{Ca}^{+2}$  ions inside the droplet further downstream resulting in the formation of crosslinked particles. In the first example of UV light initiated polymerization, Nisisako and coworkers used the T-junction configuration to controllably form droplets of hexanediol diacrylate that were then crosslinked into solid microspheres in the presence of UV light and a photoinitiator (Fig. 2b).<sup>[33]</sup> Since then a variety of crosslinking materials have been used by different groups to form polymeric microspheres under the influence of UV light (see Table 1).

## 2.5. Non-Spherical Particles

In addition to microsphere formation with fine control over size at the micrometer-scale, microfluidics has also provided the

**Table 1.** List of particles and particle assemblies created using microfluidic approaches. The articles have been organized according to the class of microfluidic methods – droplet based, flow lithography and particle assembly. The morphology, size and multiplexed (denoted by “plex”) nature of the particle along with the chemistry used are specified.

Method	Shape	Size ( $\mu\text{m}$ )	Plex	Chemistry
Droplet microfluidics (flow focusing, T-junctions, Y-junctions, co-flow)	Spherical	5–100	1	Low melting point oils [29], crosslinking acrylates or acryloyl groups [33,35], Poly(DVB) [30], PDMS with magnetic colloids [52], polysaccharides, [107,108] crosslinking acrylates doped with quantum dots [35], colloids [46], proteins [109], MIP ligands [21,90]
	Spherical	50–200	2–3	Crosslinking acrylates [43] doped with titania or carbon black [38], colloid filled [46]
	Spherical core–shell	50–200	1	Norland Optical Adhesive [28], magnetic [110], crosslinking acrylates [37], organosilicon [111]
	Spherical microporous	50–200	1	Porogen-enabled [35,53] microbubble-enabled [51], block copolymer enabled [112]
	Non-spherical (disks, rods/plugs)	20–200	1	Norland optical adhesive [34], crosslinking acrylates [35] doped with ferrofluids [45], noble metals [44]
Flow lithography (continuous flow, stop flow, interference, lock release)	Non-spherical (disks)	100	2	Crosslinking acrylates [113] filled with colloids [46]
	2D extruded	3–100	1	Crosslinking acrylates [54,55] containing colloids [70]
	2D extruded	50–200	2–4	Crosslinking acrylates [54,55,69] containing DNA [68,71], containing biodegradable polymers [114]
Particle assembly	3D Microporous	50–100	1–2	Crosslinking acrylates [61]
	3D (layered, templated, convex, concave)	50–200	1–3	Crosslinking acrylates [62,63,66]
	Particle chains	500	2–10	PS spheres [105]
	Particle assembly inside droplets/particles	20–100	1	PS spheres [3,80], silica spheres inside acrylate based particles [91]
	Assembly at droplet interface	10–100	1	Jammed with PS and PMMA colloids [86], silica particles [115]
	Field induced chains	100	1	Magnetic colloids [72–74]

unique ability to form non-spherical particles. Such particles are challenging to synthesize using traditional synthesis methods because surface tension effects lead to the formation of spheres. The natural length scale of microfluidic devices (10–1000  $\mu\text{m}$ ) has been exploited to confine micrometer-sized droplets into non-spherical shapes and then solidifying *in situ* (Fig. 3a). Doyle and coworkers<sup>[34]</sup> used this approach to synthesize plug and disk shaped particles (Fig. 3b) of varying sizes with a UV sensitive polymer (NOA 60). Droplets of NOA 60 formed at a T-junction were confined using appropriate channel geometries and then converted into solid particles by the application of a strong dose of UV light provided by an inverted fluorescent microscope. Plugs were made by shearing off droplets at low *Ca* while confining spheres in shallow channels was used to make disk shaped particles. Kumacheva and coworkers<sup>[35]</sup> used an FFD-based approach (Fig. 3e) to synthesize droplets in a variety of different oligomers before making non-spherical particles (plugs and disks) and spherical particles using both UV and thermal polymerization. In addition, composite microparticles were generated by encapsulating quantum dots, magnetic particles or fluorescent materials inside the dispersed phase before polymerization (Fig. 3f). A long, winding channel provided the required residence time to achieve solidification. The same authors also formed arrays of disks with regular periodicity by confining disk-shaped droplets in a microfluidic channel before polymerization.<sup>[36]</sup> By flowing two immiscible streams, one a monomer and the second a tuning non-polymerizable phase, through a third aqueous stream in a FFD, truncated spheres and hemispheres were also synthesized.<sup>[37]</sup> A similar approach was also used to synthesize hemispherical particles with tunable

truncated portions using a glass microfluidic device with HDDA as the monomer and silicone oil as the tuning phase.<sup>[38]</sup>

One limitation of all droplet-based methods is that all the shapes that are formed are simple deformations of spheres leading to a limited set of morphologies. Further, droplet size is typically limited to being greater than 10  $\mu\text{m}$  as this is the length scale that current low-cost device fabrication techniques based on transparency masks are limited to. However, recent efforts point to the ability to use FFD geometries and surfactant concentrations close to their critical micelle concentration (CMC) values to synthesize even smaller micrometer-sized droplets in a regime akin to the ‘tipstreaming’ regime that has been observed in unbounded flows.<sup>[39]</sup> The size of the drops here is governed by the size of the tip of the liquid jet formed and not channel dimensions. In this regime, the presence of extensional flows close to the conical tip of the emerging droplet result in gradients of surfactant concentration which aid in focusing an ejected liquid thread down to a couple of micrometers and subsequent break up into droplets.

## 2.6. Multifunctional Particles

The phenomenon of laminar flow that is seen at microfluidic length scales<sup>[40]</sup> has been exploited for a variety of applications such as micropatterning, separating materials based on differences in diffusivities and dispensing molecular gradients to cells. Laminar flow has also allowed for the formation of particles that bear stripes containing different chemical properties. Such

particles are interesting for a variety of reasons. Patchy particles with spatially segregated chemical identities can be assembled into different superstructures based on the location and size of the patch.<sup>[4]</sup> Two faced or 'Janus' particles have received wide attention since they were first discussed by de Gennes.<sup>[41]</sup> He was especially intrigued by the potential use of amphiphilic particles at interfaces. Unlike molecular surfactants which form dense, relatively impermeable films at interfaces, interfaces stabilized by such particles could be permeable because of the interstitial spaces between them leading to a veritable 'breathing' skin. A variety of methods have been proposed to synthesize such particles.<sup>[42]</sup> Among these, microfluidic methods show great promise as they allow for the synthesis of 'Janus' and particles with greater than two spatially segregated sections in one step.

Bicolored droplets containing two hemispheres – one black and one transparent – were first synthesized using a flow-focusing like geometry in a quartz glass microfluidic device.<sup>[33]</sup> Two isobornyl acrylate streams – one doped with carbon black (black) and the other with titanium dioxide (white) – in parallel laminar flow were forced through a flow-focusing like geometry to form droplets containing two distinct sections (Fig. 4a). These droplets were then polymerized into solid particles (Fig. 4b) using thermal polymerization. After this first demonstration of these two-faced, Janus particles, a number of others have also formed such particles in microfluidic devices. Coflowing immiscible monomers (Fig. 4c), which results in a sharp interface between the different phases, were used to form multifunctional droplets that were then converted into Janus and ternary particles (Fig. 4d) in the presence of UV light.<sup>[43]</sup> The surface properties of the monomers and their interaction with the material of the microchannel used were found to be critical to their ability to form ternary particles of a desired structure.<sup>[43]</sup>

## 2.7. Composite Particles

The functionality of particles synthesized using microfluidics can be increased by the incorporation of dyes, nanoparticles, quantum dots, biomolecules etc. into the dispersed phase before polymerization. A variety of materials including fluorescent dyes, CdSe quantum dots, porogens, magnetic particles and liquid crystals were incorporated into microparticles composed of a UV light sensitive system comprising TPGDA.<sup>[35]</sup> Gold and silver particles as well as dye-doped polystyrene microrods were synthesized in a segmented flow microfluidic device using thermal polymerization.<sup>[44]</sup> Spherical and non-spherical poly (ethylene glycol) (PEG) particles containing homogeneously

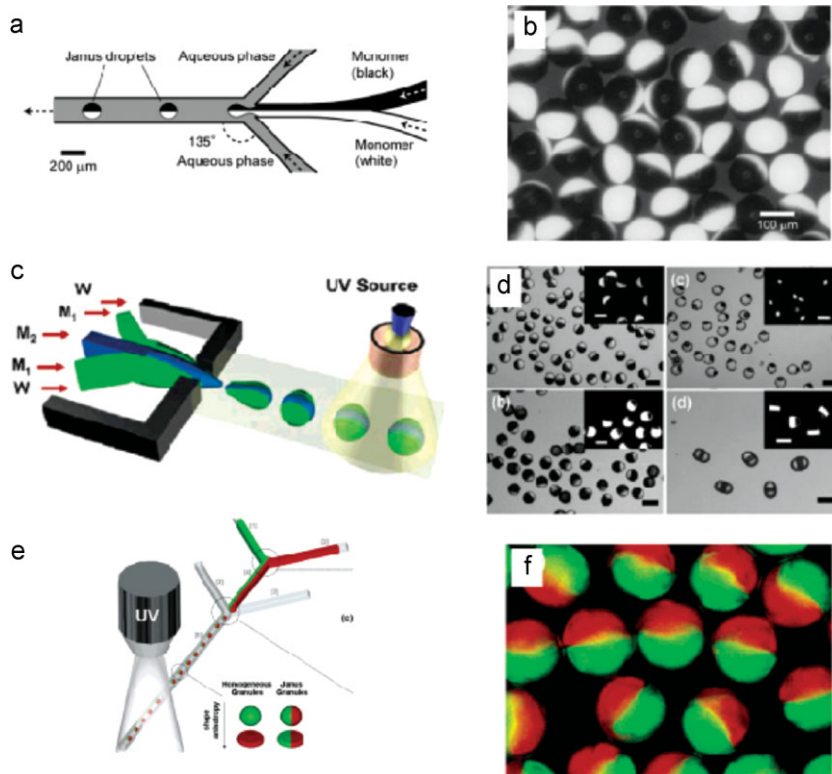


**Figure 4.** Janus and ternary particles synthesized using droplet-based particle formation in a microfluidic device. a) FFD-like geometry first used for the synthesis of Janus particles. Reproduced with permission from [93]. b) Janus particles synthesized using the device in a). Reproduced with permission from [93]. c) FFD geometry used for the synthesis of complex Janus and ternary particles [43]. d) Janus and ternary particles with tunable anisotropy formed using the device in c). e) Colloid-filled Janus hydrogel granules formed in a FFD like microfluidic device. Reproduced with permission from [46]. Copyright 2005 American Chemical Society. f) Janus granules synthesized using the device in e).

encapsulated magnetic nanoparticles were also synthesized in a microfluidic T-junction device (Fig. 3d).<sup>[45]</sup> The device used an aluminum foil reflector to accomplish the homogeneous polymerization of the microparticles which is otherwise difficult to achieve because of the strong absorption of UV light by the magnetic nanoparticles. Lewis and coworkers formed colloid-filled hydrogel particles by combining the ability to encapsulate colloidal granules and produce Janus particles at the same time in one microfluidic device (Fig. 4e).<sup>[46]</sup> Acrylamide-based hydrogel pre-polymer that was concentrated with fluorescently labeled 500 nm silica spheres was used to form droplets in an FFD like geometry. These droplets were then photopolymerized to form granules that were either homogeneous (discoids and spheres) or heterogeneous Janus particles (Fig. 4f).

## 2.8. Core-Shell and Porous Particles

In addition to O/W and W/O emulsion droplets, microfluidic devices have been exploited elegantly to synthesize more complex W/O/W and O/W/O emulsion droplets.<sup>[47]</sup> Such droplets, with multiple internal layers, are extremely useful for synthesizing



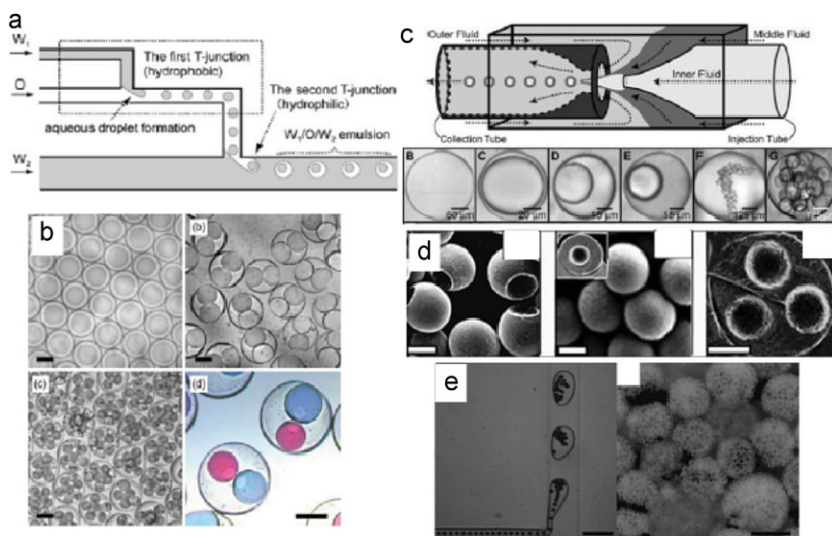


**Figure 5.** Core shell particles synthesized using droplet-based microfluidic devices. a) Double emulsion droplets being formed from a two-stage T-junction based microfluidic device. Reproduced with permission from [48]. Copyright 2004 American Chemical Society. b) Droplets from a) containing multiple monodisperse inner droplets [48, 104]. c) Glass capillary based device used to form monodisperse, complex emulsion droplets. Reproduced with permission from [28]. Copyright 2005 American Association for the Advancement of Science. d) Core shell particles formed using an FFD device. Reproduced with permission from [37]. Copyright 2005 American Chemical Society. e) Highly porous particles formed using microbubble-in-water-in-oil emulsion droplets. Reproduced with permission from [51].

particles for encapsulation applications and to serve as surrogates for cells or to create giant vesicles. By using two T-junctions, one bearing hydrophilic and the other bearing hydrophobic properties (Fig. 5a), Nisisako and coworkers synthesized double emulsion droplets containing a controllable numbers of encapsulated droplets (Fig. 5b) in a glass microfluidic device.<sup>[48]</sup> A similar configuration was implemented in a PDMS microfluidic device by Tabeling and coworkers.<sup>[49]</sup> A plasma polymerization technique in conjunction with suitable masking was used to permanently convert only one of two T-junctions in a device to a hydrophilic state while leaving the other in its native hydrophobic state. Both W/O/W and O/W/O emulsions were formed using this method. Kumacheva and coworkers<sup>[37]</sup> used a polyurethane-based FFD to form complex emulsion droplets by flowing a combination of two immiscible fluids, silicone oil and a monomer, through a third aqueous phase. The authors obtained very precise control over core and shell thickness of the droplets as well as the number of internal droplets in each emulsion droplet by varying the ratio of the flow rates of the different phases. The complex droplets formed were polymerized to freeze in the core-shell structure (Fig. 5d) of the complex droplets formed.

Weitz and coworkers used a custom fabricated glass capillary device (Fig. 5c) to synthesize double emulsion droplets that contained a controllable number of one or more inner droplets in one single step.<sup>[28]</sup> The device consists of two cylindrical glass capillary tubes nested within a square glass tube. One cylindrical tube is used to pump the innermost fluid while the middle fluid is pumped through the outer coaxial region surrounding the cylindrical tube. The outermost fluid is simultaneously pumped through the outer coaxial region from the opposite direction, and

all fluids are forced through the exit orifice formed by the remaining inner tube. The flow passes through the exit orifice and subsequently ruptures to form drops; however, the coaxial flow can maintain its integrity and generate double emulsions. W/O/W emulsion droplets that contained a photosensitive monomer in the oil phase were then used to synthesize hollow particles by photopolymerization. The same group also used the capillary based generation of double emulsions to form gel-shell structures with a controllable number of inner droplets.<sup>[50]</sup>

More recently Stone and coworkers synthesized porous polacrylamide microparticles in a two-step process.<sup>[51]</sup> In the first step, microbubble-in-water emulsion droplets were synthesized in a FFD. This gaseous phase was then passed through either a second FFD or a T-junction device with oil as the continuous phase to form microbubble-in-water-in-oil emulsion droplets (Fig. 5e). By including photopolymerizable acrylamide solution in the aqueous phase and subsequent photopolymerization, highly porous particles were formed. Core-shell particles comprising an elastic PDMS shell that encases a ferrofluid have also been synthesized and show magnetostrictive effects.<sup>[52]</sup> Kumacheva and coworkers

have also used porogens encapsulated inside the monomer mix before polymerization in order to form porous<sup>[35]</sup> and macroporous particles.<sup>[53]</sup> The porogen is an organic solvent that is washed out after crosslinking, leaving hollow spaces inside the particle

### 3. Synthesis Using Flow Lithography Methods

Until now, we have covered particle synthesis methods that have relied on the controlled formation of droplets inside microfluidic devices. In such methods, particle shape is restricted to spheres or shapes that result from the simple geometrical deformations of spheres, like discoids, plugs or hemispheres. Further, the necessity to emulsify a droplet before polymerization requires optimizing the surface chemistry of the dispersed phase, continuous phase and the device so that droplets can be formed in a continuous and reliable manner.

The Doyle group recently introduced a new class of microfluidic methods that uses photolithography to define particle shape.<sup>[54,55]</sup> In contrast to the droplet-based multi-phase flow methods, these lithographic techniques rely on transparency masks to provide shape-definition. The technique can be conveniently implemented on an inverted microscope using projection photolithography.<sup>[56]</sup> Arrays of mask-defined polymeric particles are patterned into a UV light sensitive pre-polymer before being flowed out of the microfluidic device. The ability to create free-standing particles using flow lithography is based on the inhibition of free radical polymerization reactions

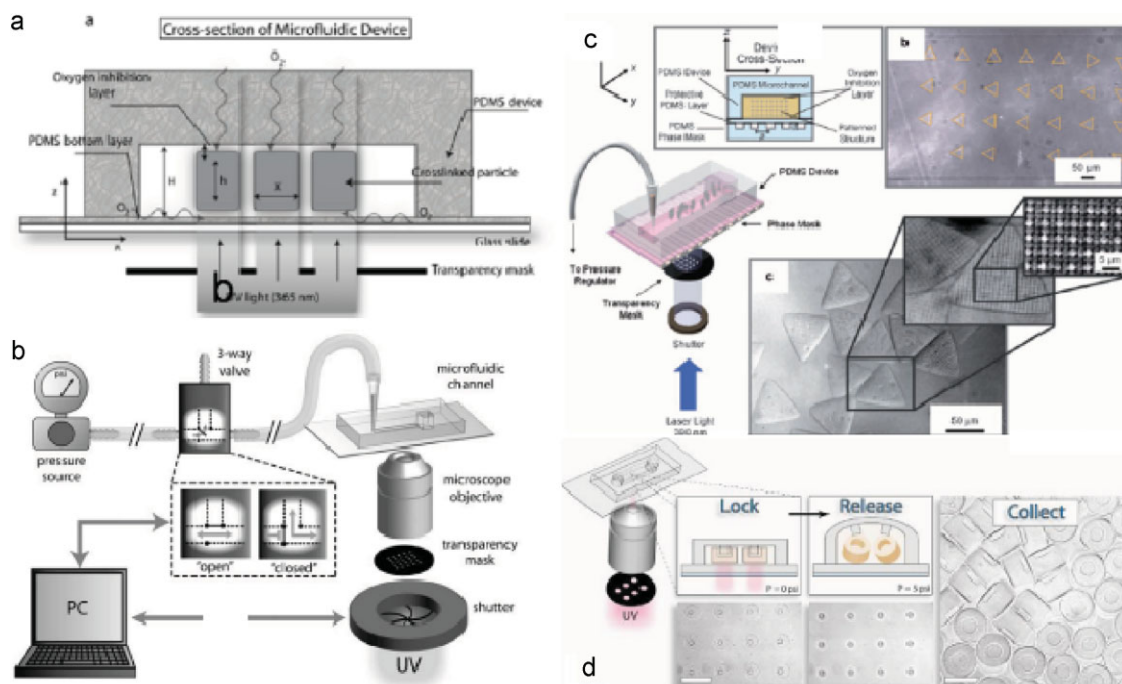


**Figure 6.** Flow Lithography Setup. a) Cross-section of an all PDMS microfluidic device used in Flow Lithography. Mask defined shapes are shown crosslinked in the center of the device along with the oxygen inhibition layer that permits them to flow out. Reproduced with permission from [58]. Copyright 2008 American Chemical Society. b) Setup used for Stop Flow Lithography (SFL). A 3-way solenoid valve permits rapid stopping and starting of the flow before and after polymerization. Reproduced with permission from [55]. Copyright 2007 Royal Society of Chemistry. c) Stop Flow Interference Lithography (SFIL) setup showing a phase mask integrated into the PDMS device as the bottom layer. An array of triangles is produced that contain internal porosity. Reproduced with permission from [61]. d) Schematic of Lock-and-Release Lithography used for the synthesis of more complex 3D and overlapped particles [62].

at the surface of the PDMS devices used. This inhibition is caused by oxygen from the surrounding air freely diffusing in through the porous walls of the PDMS device. Oxygen is able to inhibit free radical photopolymerization reactions by reacting with radical species to form chain terminating peroxide molecules.<sup>[57]</sup> The oxygen consumed in these reactions is replenished by the oxygen that is constantly diffusing in through the PDMS walls (Fig. 6a). This competing reaction-diffusion process ensures that there is an uncrosslinked “lubrication layer” close to the walls of the PDMS device, which enables the particles to flow out without sticking. A model to study the phenomenon of oxygen inhibition at microfluidic device length scales was recently proposed and experimentally validated.<sup>[58]</sup> One advantage of flow lithography is that it enables photolithography to be performed on low viscosity liquids and suspensions that are not always amenable to being spin-coated, a pre-requisite before traditional photolithography is performed. This opens up the possibility of extending photolithography from being performed on only photoresist materials to several new polymers including bio-friendly materials. Prior to flow lithography, others had polymerized a continuous phase of monomer passing through a microfluidic device to synthesize tubes of polymer<sup>[59]</sup> or used masks to synthesize hydrogel based valves<sup>[60]</sup> that were embedded inside a microfluidic device. However, flow lithography was the first demonstration of arrays of arbitrary mask defined particles being formed and flowed out of a microfluidic device

### 3.1. Continuous and Stop-Flow Lithography

In the first of these processes described, Continuous Flow Lithography (CFL), photolithography was performed in a continuously flowing stream of PEG-diacrylate (DA).<sup>[54]</sup> Transparency mask defined shapes were patterned into a continuously flowing oligomer stream which flowed the particles away as they were formed. Like traditional lithographic methods, the process was versatile enough to synthesize any 2D extruded shape. The theoretical resolution of the method is roughly equal to the wavelength of light used although features down to only 3  $\mu\text{m}$  were synthesized using CFL.

Because particles are formed in a flowing stream of oligomer, particle throughput cannot be increased without compromising resolution. When high flow rates are used to increase throughput, unacceptable smearing and deformation of particle features occurs. When low flow rates are used to increase resolution, particle throughput is adversely affected. To address these deficiencies, Stop Flow Lithography (SFL), was developed.<sup>[55]</sup> A flowing stream of oligomer is stopped (Fig. 6b) before polymerizing an array of particles into it, providing for much improved resolution over particles synthesized in flow. The formed particles are then flushed out at high flow rates before the cycle of stop-polymerize-flow is repeated. SFL lead to particle features down to 1  $\mu\text{m}$  and up to a thousand times improvement



in throughput compared to CFL. In addition, it was found that even for the synthesis of particles with multiple sections, SFL lead to sharp interfaces between the different sections because a high  $Pe$  flow could be used right before stoppage and subsequent polymerization.

### 3.2. Stop Flow Interference Lithography

One limitation of traditional lithographic methods is that all the features that are formed have a 2D extruded shape. Control over particle features in the third dimension have been obtained using such methods as two photon microscopy, direct 3D writing, colloidal assembly or interference lithography. Of these methods interference lithography offers certain advantages such as large area coverage, and control over geometrical parameters such as symmetry and volume fraction of the structures formed. In interference lithography, laser light passing through a phase mask (a mask that induces phase differences in the light exiting the mask) causes peaks and troughs in light intensity in the direction of propagation of light. This causes the formation of particles with 3D structures. By combining phase mask based interference lithography with SFL, a new process called Stop Flow Interference Lithography (SFIL) was developed (Fig. 6c).<sup>[61]</sup> This method enabled the formation of particles with predictable internal 3D structures in one shot. Such particles could be especially useful in sensing applications where high surface-area-to-volume ratios are desired.

### 3.3. Lock and Release Lithography

Very recently, a new process that utilizes the deformation of PDMS devices under external pressure was used to synthesize a wider class of 3D dimensional and multifunctional particles.<sup>[62]</sup> 3D PDMS molds containing positive relief structures protruding from the ceiling are used to synthesize particles that would normally be 'locked' in a flow. These particles are then forced out of the microfluidic device by using a high pressure pulse that deforms the PDMS device and releases the particles (Fig. 6d). Composite particles are also created by flowing in one solution, locking a particle in place using one mask, flowing in a second solution and then forming an overlapped region around the first chemistry using a different mask. A powerful feature of this approach is that it allows the synthesis of multifunctional particles where the distinct sections are not restricted to being parallel stripes but can include more complicated overlaps. (Fig. 7g) Kwon and coworkers have also used methods based on the deformation of PDMS membranes to synthesize complex 3D structures that are attached to a surface.<sup>[63]</sup>

### 3.4. Non-Spherical Particles

A variety of 2D extruded shapes were synthesized in the first demonstration of CFL.<sup>[54]</sup> These included triangles, circles, squares, curved shapes, ring shapes and several others (Fig. 7a). The range of shapes formed greatly expands on that available

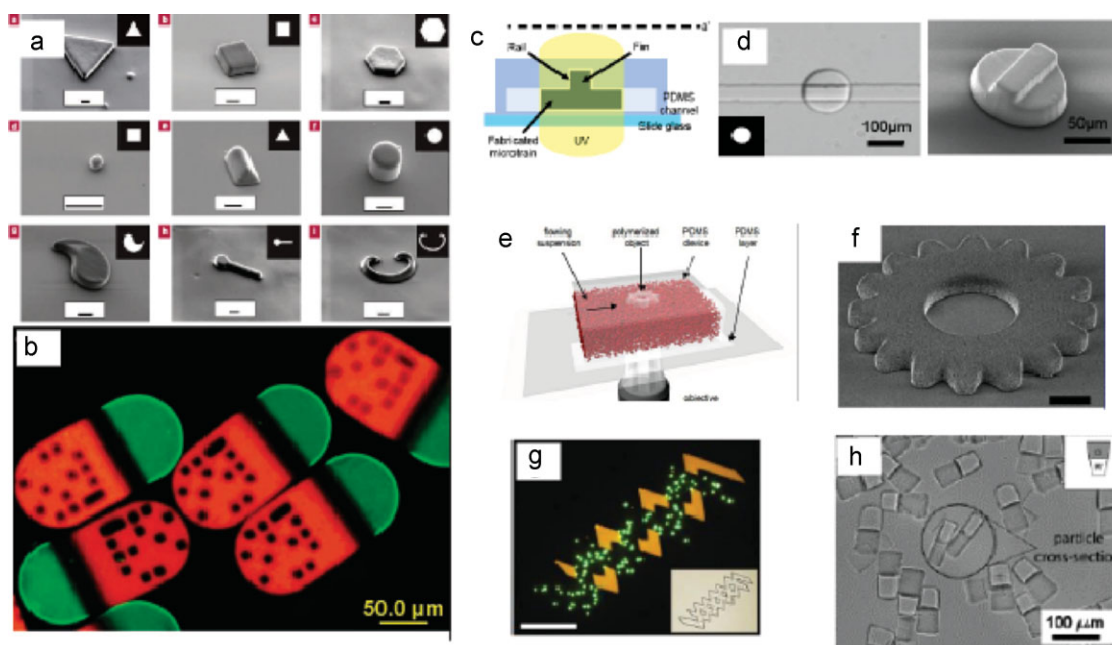


**Figure 7.** Particle morphologies synthesized using flow lithography based processes. a) A variety of 2D extruded shapes produced using CFL. Reproduced with permission from [54]. Copyright 2006 Macmillan Publishers. b) Barcoded particles used for the assembly of viruses that contain three distinct sections. Reproduced with permission from [71]. Copyright 2008 American Chemical Society. c) Schematic of a non-rectangular cross-section of a PDMS device used for the synthesis of 3D particles and d) particles with a 3D cross section synthesized using this method. Reproduced with permission from [67]. Copyright 2008 Macmillan Publishers. e) SFL based synthesis of colloid granule containing microgears and f) sintered microgear formed from the process in e). Reproduced with permission from [70]. g) 3D particle with complex patches of fluorescent green and yellow formed using LRL [62]. h) Amphiphilic particles formed from two immiscible phases using CFL. Reproduced with permission from [69]. Copyright 2008 American Chemical Society.

from droplet-based microfluidics although the synthesis of simple spherical particles is not possible. The smallest feature size reported was 3  $\mu\text{m}$ . SFL, an improvement on CFL, was then used to synthesize arrays of particles with feature sizes down to 1  $\mu\text{m}$ .

Flow lithography is most commonly implemented by inserting a mask containing the desired shape into the field stop plane of an inverted microscope. This restricts the ability to easily change shape on demand. Digital micromirror devices (DMDs) can be pre-programmed to change their mask pattern and have been used in lithography applications with modest spatial resolution requirements in order to reduce the fabrication cost and turnaround time of the photomasks. The integration of DMDs with flow lithography allows particle size and shape to be changed at will.<sup>[64]</sup> Kwon and coworkers synthesized microparticles with a resolution down to 1.54  $\mu\text{m} \times 1.54 \mu\text{m}$  using a DMD device integrated into an optical microscope.<sup>[65]</sup> Particles with varying shapes in the size range of 50–100  $\mu\text{m}$  and composed of PEG-DA were synthesized using this method.

Coflowing immiscible streams in a microfluidic device share a curved interface with each other. The curvature of this interface depends on the interfacial tension between the two liquids and the solid-liquid surface tension between the PDMS and the liquids. This curvature effect has been exploited by Doyle and coworkers to synthesize 3D particles with concave and convex faces.<sup>[66]</sup> Multiple immiscible fluids, some of which contained photoinitiator that enabled polymerization and others without photoinitiator that functioned as tuning fluids were used to synthesize particles with tunable curvature by polymerizing across the interface of these coflowing liquids.

An important class of particles that is difficult to synthesize using single-step photolithography is 3D particles. The first step towards the synthesis of such particles was made recently by exploiting a combination of CFL and 3D PDMS devices. Particles containing rails were synthesized using this method as depicted in Figure 7c and d.<sup>[67]</sup> The technique of lock and release lithography allows for the synthesis of even more complex 3D particles.<sup>[62]</sup>

### 3.5. Multifunctional Particles

Like in droplet-based methods, the laminar flow seen at microfluidic device length scales has been used to synthesize multifunctional particles in flow lithography based processes too. An additional practical advantage over droplet-based methods is that particles with more than three different sections are readily synthesized using flow lithography. For the same size, a particle with a greater number of laminar sections than one with fewer sections will tend to mix by diffusion more quickly because of the reduced length scale per section. This means a particle must be polymerized almost at the same instant after formation to preserve the distinct sections. In SFL, polymerization can be performed soon after strip formation and stoppage whereas droplet based techniques typically have slightly longer residence times before encountering polymerization.

High  $Pe$  flows (where the ratio of convection to cross stream diffusion is high) which lead to sharp interfaces between different

sections may be used in SFL as opposed to CFL where only low  $Pe$  flows can be used. As compared to traditional photolithographic patterning, the combination of flow with photolithography also allows for the ability to synthesize multi-functional particles in one single step. The fluids in question can be either miscible or immiscible fluids and up to seven different streams have been coflowed before polymerization. Extruded bar shaped particles with two different sections – one a fluorescent PEG-DA and the other PEG-DA alone – were synthesized using CFL by exploiting laminar flow.<sup>[54]</sup> When using miscible streams, the low flow rates that CFL requires result in non-sharp interfaces between distinct sections of the particle. This problem was mitigated in SFL by using high  $Pe$  flows which are stopped just before polymerization resulting in sharp interfaces.<sup>[55]</sup> Bar-shaped particles with three distinct sections that showed markedly sharper interfaces than in CFL were synthesized. Multifunctional encoded particles that contained a unique lithographically patterned barcode on one section and a DNA probe oligomer on the other were synthesized using SFL (Fig. 7b).<sup>[68]</sup> Immiscible streams in laminar coflow were used to synthesize particles with ‘amphiphilic’ properties (Fig. 7h).<sup>[69]</sup> A hydrophilic stream that was an aqueous solution of PEG-DA and a hydrophobic stream that contained TMPTA were flowed parallel to each other before wedge-shaped particles were formed, five at a time, across the interface. More recently, LRL was used to form complex particles with multiple distinct and overlapping sections that could not be formed using simple laminar flow based lithography.<sup>[62]</sup> In Figure 7g is shown a particle synthesized using such an overlap.

### 3.6. Porous Particles

The pore size of the particles obtained using cross-linking materials like PEG-DA is usually too low (on the order of a few Å) for the entry or release of large molecules like proteins. It was found that even smaller molecules like DNA oligomers containing around 20 bases were unable to penetrate such particles.<sup>[68]</sup> While porogenic materials may be introduced into particles to obtain porous structures, such materials are usually organic solvents that are incompatible with most relevant biomolecules. Very porous particles may be synthesized by the addition of glycerol or PEG solutions along with using PEG-DA molecules that contain long PEG spacers.

Alternately, SFIL has been used for the synthesis of particles with very controlled 3D porosity in the range of 1–2  $\mu\text{m}$  (Fig. 6c). The advantage of using this method is that geometrical porosity is very finely controlled which will lead to greater repeatability in sensing applications. The synthesis of ‘fully-open’ structures has not yet been possible because the polymers that are being used have not been optimized for such applications. Photoresist like materials which have separate acid generation (on exposure) and crosslinking (on baking) steps lead to truly open structures. Such materials must be investigated in SFIL to obtain truly open structures.

### 3.7. Composite Particles

SFL has been used for the synthesis of ceramic micro components. Mask defined structures were formed in a hydrogel

film containing silica nanospheres (Fig. 7e). The pre-polymer had to be index-matched to the silica nanospheres ( $n = 1.46$ ) using a mixture of dimethyl sulfoxide (DMSO,  $n = 1.48$ ) and water ( $n = 1.33$ ) in order to avoid absorption and scattering events that would deteriorate the polymerization efficiency. The formed particles were then sintered in a furnace to form ceramic microcomponents with a glassy texture (Fig. 7f).<sup>[70]</sup> Virus, such as Tobacco Mosaic Virus (TMV), have also been readily incorporated into bar-coded particles formed using SFL.<sup>[71]</sup>

#### 4. Microparticle Synthesis Using Colloidal Assembly in Microfluidic Devices

A third category of processes involves those that use microfluidic devices to assemble, manipulate or alter pre-existing microparticles into more complex structures or “supraparticles”. Such processes have the advantage of introducing a 3D character into the structures formed. Some of the earliest microfluidic efforts in this area come from Furst and Gast<sup>[72]</sup> who assembled magnetic particles under an applied magnetic field into linear chains between two surfaces, one of which was a semi-permeable membrane. They subsequently infused a cross-linking agent across the membrane to form monodisperse linear superparamagnetic chains (Fig. 8e and f). This simple but effective fluidic device allowed for controlling both the chain height (geometrically) and facile introduction of cross-linking chemicals. Similar strategies were explored by Hatton and Laibinis to form both rigid and flexible superparamagnetic chains.<sup>[73,74]</sup>

While the aforementioned colloidal aggregates were assembled by magnetic fields, other groups have used surface tension forces in a droplet to form complex structures. Velev and Kaler<sup>[75]</sup> showed that microdroplets suspended on fluorocarbon oils could be used as compartments to crystallize colloids via controlled solvent evaporation into structured spheres, ellipsoids and toroids. Velev later extended this technique to create microreactors which move the droplets using electric fields.<sup>[76]</sup> Exotic structures such as ‘eyeballs’, stripes and capsules could be made with this process. The works of Velev and Kaler produced supraparticles of size  $\approx 500 \mu\text{m}$  which contained many colloids per particle (large  $N$ ). A broader class of supraparticle morphologies result when the emulsion droplets contain only a few colloids (e.g.,  $N \approx 4-20$ ). Manoharan and Pine synthesized such small  $N$  clusters using bulk emulsion templating which produces a broad mixture of cluster sizes.<sup>[77,78]</sup> Yi, Quake, Pine, Thorsen and Pine<sup>[79,80]</sup> built off this concept and used two phase flows to produce more monodisperse colloid-containing droplets. Evaporation of the solvent in the dispersed phase then drove the assembly of the colloids into clusters (Fig. 8a and b).

Xia used open microchannels and other relief structures as geometric templates to pattern spherical colloids during dewetting of the solvent.<sup>[81-83]</sup> They created a wide range of homo-aggregate (one colloid type) structures ranging from linear zigzag chains to rings to polyhedral clusters both at the micro and nanoscale. Limited types of controlled hetero-aggregates can also be formed with this method using a multistep process. Solomon and coworkers recently developed microreactors which also use geometric templates.<sup>[84]</sup> Colloids are packed into dead-end production channels (with a weir at one end) and then thermally

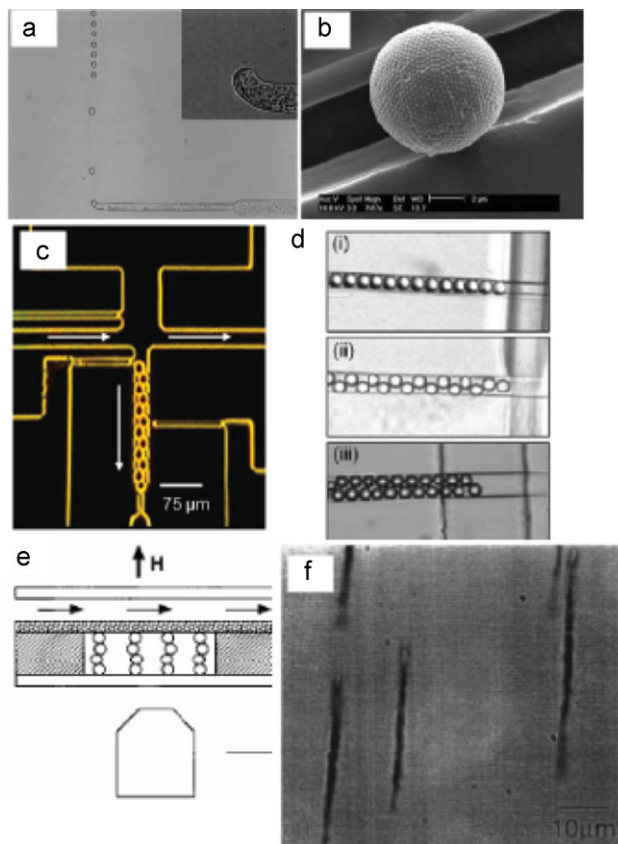


**Figure 8.** Particle assembly in microfluidic devices. a) A particle laden phase being emulsified into droplets at a T-junction and b) the resultant colloid assembly formed on evaporation. Reproduced with permission from [80]. c) A constricted channel used to synthesize linear zig-zag colloidal ‘molecules’ and d) brightfield images showing the differentiated assembly of particles in channels of different dimensions. Reproduced with permission from [105]. Copyright 2008 American Chemical Society. e) Colloidal magnetic chains synthesized in a micrometer-sized channel in the presence of magnetic field and f) the chains in an externally applied magnetic field. Reproduced with permission from [72]. Copyright 1998 American Chemical Society.

fused together (Fig. 8c and d). The great advancement of their technique is that through programmed microfluidic control they can deliver colloids of multiple types (e.g., ‘A’ and ‘B’) into the production zone with a specified order. This allows for precise synthesis of hetero-aggregates, such as homogeneous populations of linear chains with colloid order A-B-AA-B etc. Stone and coworkers have exploited the assembly of colloids at fluid interfaces to synthesize non-spherical bubbles<sup>[85]</sup> and ‘armored’ droplets<sup>[86]</sup> whose surfaces are jammed with particles. These composite materials have distinct mechanical properties, providing a plastic response to inhomogeneous stresses and an elastic response to small homogeneous stresses.

#### 5. Applications

The past few years have seen a spurt in the introduction of fabrication methods for polymeric microparticle synthesis and



assembly in the academic literature. While several innovative methods have been developed and others will doubtless follow, it is instructive to take stock of the applications (both demonstrated and proposed) that some of these particles have been put to. It must also be pointed out that most of these applications are in the proof-of-concept stage in academic laboratories and can be transferred to current industrial practice only upon the performing of suitable benchmarking studies and technology validation.

### 5.1. Microfabricated Components – Polymers, Silicon, Glass

The synthesis of precisely defined microparticles and components that are composed of inorganic materials like silica, titania and ceramics remains a challenge. These particles could be used as microgears or micromixers inside microelectromechanical-system (MEMS) devices.<sup>[87]</sup> Flow lithography provides an elegant solution to the synthesis of such materials. Shepherd et al. have shown the synthesis of glassy micro-gears (Fig. 7f) by using SFL to synthesize refractive index matched polymer gel containing colloidal granules that were then converted to oxide and non-oxide structures through sintering at 1150 °C for 3–10 h.<sup>[70]</sup> Along with complementary technologies like optical tweezers, such microfabricated components could be used for the assembly of more complex microchips that contain multiple different components. Very recently, Bartolo and coworkers demonstrated the use of a ‘soft’ microflow sensor fabricated into a device using SFL.<sup>[88]</sup> The sensor was used to track flow rates inside a microfluidic device by measuring the extension of a soft spring made using a hydrogel polymer. The sensor had a dynamic range of 3–4 orders in magnitude and could track flow rates down to as low as  $\text{nl min}^{-1}$ .

### 5.2. Particle Sensors – Encoded Particles

One of the most promising applications of the complex particles synthesized using microfluidic devices is in particle diagnostics.<sup>[2]</sup> Particle based assays are expected by some to replace traditional plate-based assays like ELISAs for rapid, high throughput, multiplexed analysis of genomic, proteomic and metabolomic analytes. The key challenge in multiplexing is to be able to generate large numbers of particle codes that are both unique and easily readable. SFL was used to generate particles, one half of which can have any one of millions of unique square pattern signatures while the other half contains a probe molecule that is linked to the unique signature.<sup>[68]</sup> Particles suspended in a solution containing the molecules of interest are used as probes which can detect these target molecules through a very specific interaction like DNA base-pairing. Particles are then passed through a detector where their unique barcode reveals the molecular signature while the probe-detector complex reveals the presence and quantity of the target molecule (Fig. 9g). An advantage over current systems is the ability to use only one fluorescent molecule for both target identification and quantification. The technique was used to detect DNA oligomers down to the pM level. Recently, others have used the different shapes

provided by CFL as a means of providing multiplexing for the detection of a few different proteins. The use of Molecularly Imprinted Polymers (MIP) is an emerging technology for the specific spatial sensing of ligands using polymeric templates.<sup>[89]</sup> Polymeric substrates that contain a specific templating ligand are first formed before the template is selectively removed leaving cavities that can specifically sense the ligand molecule. Microfluidic droplet based methods have been used for the synthesis of very monodisperse MIP beads that can be used to selectively separate a ligand from a mixture containing several similar molecules.<sup>[90]</sup>

### 5.3. Building Blocks for Assembly and Photonic Crystals

Material scientists envision that the materials of the future will be built through self-assembly. In this scheme that is inspired by nature, large numbers of building blocks will build themselves into complicated superstructures through instructions that are coded in their own structures. In such applications, precisely designed building blocks are essential to increase the ease of assembly.<sup>[4]</sup> Non-spherical particles lead to a much wider range of crystal structures than spherical particles in such materials. Amphiphilic, wedge-shaped particles synthesized using CFL were assembled into micelle-like structures to demonstrate the utility of precisely shaped building blocks in assembly applications (Fig. 9b). One such application that is being actively pursued today is the building of photonic devices through the self-assembly of colloidal particles encapsulated inside droplets synthesized using microfluidics. Double emulsion droplets encapsulating arrays of colloidal particles were used to form colloidal crystal arrays in a coflowing capillary-based microfluidic device.<sup>[3]</sup> The outer shell phase of the double emulsion was a photocurable resin that was photopolymerized downstream of the fluidic channel within 1 s after drop generation (Fig. 9e). Such particles showed diffraction patterns that were very distinct from conventional film type arrays of colloids and were independent of the orientation of the spherical surface. Yang and coworkers also synthesized colloidal suprastructures by incorporating silica nanospheres inside a photopolymerizable resin.<sup>[91]</sup> Droplets containing nanospheres were formed using a capillary based coflow configuration and photopolymerized into solid microspheres using UV light from a microscope. By varying the size and concentration of the nanospheres, the authors were able to obtain different wavelengths of reflected light from samples containing such microspheres. For instance, varying the fraction of encapsulated 165 nm nanospheres through  $\varphi = 0.33, 0.25$  and  $0.17$  changed the wavelength of reflected light to blue green and red respectively (Fig. 9f). Such particles could find use in applications like electronic paper (e-paper), photonic crystal sensors and light emission modulators.

Bibette and coworkers synthesized chains of 350 nm sized magnetic colloids by bridging them together using polyacrylic acid based linkers.<sup>[92]</sup> The particles were loaded in a 200  $\mu\text{m}$  wide microchannel and assembled together in the presence of a magnetic field (Fig. 9j). Such chains were used as mechanical sensors to measure the bending rigidity of the linker molecules used. Janus particles with distinct black and white sections were

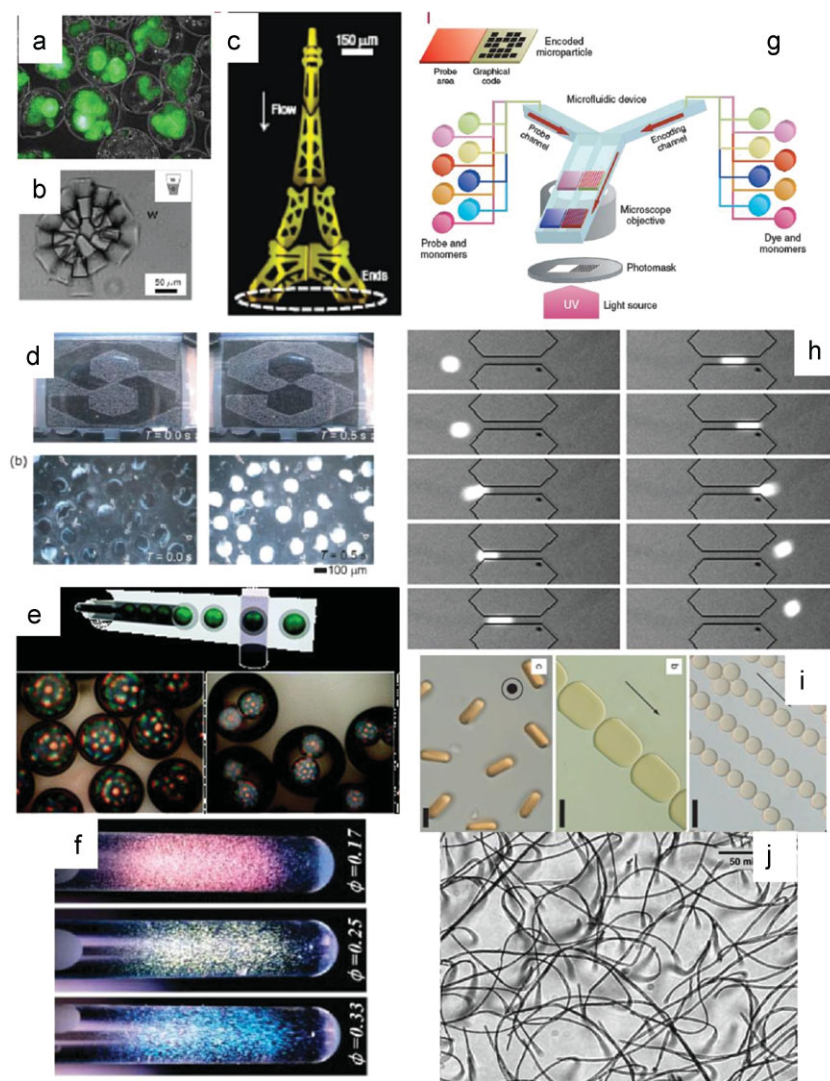


**Figure 9.** Applications of particles synthesized using microfluidic processes. a) CHO/NK4-GFP cells encapsulated inside alginate particles produced using a microfabricated nozzle. Reproduced with permission from [94]. Copyright 2007 Springer. b) Assembly of amphiphilic particles to form micelle like structures in water. Reproduced with permission from [69]. Copyright 2007 American Chemical Society. c) Complex assembly of particles built using guided assembly on rails. Reproduced with permission from [67]. Copyright 2008 Macmillan Publishers. d) Janus particles used in an e-paper application. Reproduced with permission from [93]. e) Photonic crystal arrays encapsulated inside a resin shell and synthesized using colloidal assembly in microfluidics generated droplets. Reproduced with permission from [3]. Copyright 2008 American Chemical Society. f) Aqueous dispersions of photonic microspheres containing different volume fractions of silica nanospheres. Different fractions filter different wavelengths from a white light source. Reproduced with permission from [91]. g) Encoded particles used for massively multiplexed nucleotide diagnostics. Reproduced with permission from [106]. Copyright 2006 Macmillan Publishers. h) Squishy particles which mimic red blood cells generated using SFL deform as they pass through a narrow channel. Reproduced with permission from [99]. Copyright 2008 Micro Total Analytical Systems ( $\mu$ TAS). i) Magnetic spheroids align in an externally applied magnetic field. Reproduced with permission from [45]. Copyright 2008 Royal Society of Chemistry. j) Flexible magnetic filaments used to probe the biomechanical properties of molecules. Reproduced with permission from [92]. Copyright 2003 American Physics Society.

electrically actuated to display a particular section on demand.<sup>[93]</sup> These two-faced particles could then be used as the constituents of electronic paper, a display technology which some believe could replace paper in a number of applications in the future (Fig. 9d).

Very recently, CFL performed with a dynamic mask provided by a digital micromirror device was used to assemble complex structures comprised of micrometer-sized building blocks.<sup>[67]</sup> Kwon and coworkers exploited the oxygen inhibition layer to flow particles along guided rails to their destination. Complex structures composed of more than 50 microstructures (each sized smaller than  $50\ \mu\text{m}$ ) were fluidically self-assembled with zero error (Fig. 9c). The particles were able to assemble accurately while overcoming strong interfacial tension forces between streams. Such complex structures could be used in tissue engineering applications. Non-spherical magnetic particles show rich behavior in the presence of external magnetic fields. Their shape induced anisotropy leads to magnetic chains that contain particles in a preferred orientation that minimizes their energy (Fig. 9i).

#### 5.4. Cell and Protein Encapsulation

The encapsulation of living cells that have been genetically modified to secrete a certain protein could prove useful as a means of therapy. Alginate beads, prepared by extrusion through a micro nozzle, were encapsulated with Chinese Hamster Ovary (CHO) cells that secreted marker proteins like Green Fluorescent Protein (GFP) and then encapsulated inside an outer shell comprising poly-L-lysine and alginate.<sup>[94]</sup> The inner core was then dissolved to enable cell growth. Cell encapsulated beads (Fig. 9a) could be formed in the size range of  $120\text{--}300\ \mu\text{m}$  (CV of 7.5%) with smaller beads providing better cell growth and protein secretion. Encapsulating cells within hydrogels is also important for generating tissue constructs that can control the micro-environment interactions in order to mimic native tissue architecture and direct cellular differentiation and organization. Stop flow lithography was used to generate PEG micro-particles containing encapsulated NIH-3T3 mouse fibroblast cells.<sup>[95]</sup> Cell viability was ascertained using a live-dead assay and was optimized by varying the concentrations of pre-polymer (PEG-DA), photoinitiator (Irgacure 2959) and accelerator (NVP). Such cell encapsulated particles could later be assembled to form more complex 3D structures. Biodegradable polymeric microspheres are convenient agents for the controlled release of bioactive species in drug delivery applications.<sup>[96,97]</sup> Micromachined devices have been used for the solvent extraction based synthesis of such microspheres. Gander and coworkers synthesized PLGA

(poly (lactic-co-glycolic acid)) microspheres encapsulated with bovine serum albumin (BSA). PLGA dissolved in dichloromethane (DCM) and containing emulsified BSA was extruded through an outlet slit into a PVA containing aqueous phase before the DCM was extracted resulting in the formation of microspheres in the size range of 8–29  $\mu\text{m}$  with a relatively large size distribution.<sup>[98]</sup>

### 5.5. Cell Surrogates

In many applications, particles synthesized using microfluidic techniques can serve as surrogates for cells. For instance, Doyle and coworkers used SFL to synthesize very loosely crosslinked 'squishy' particles that could serve as surrogates for red blood cells (RBCs).<sup>[99]</sup> When the ratio of the crosslinker PEG-DA to PEG (MW 700) in these mixtures was appropriately tuned, the RBC-like particles were soft enough to deform as they passed through narrow channels (Fig. 9h). Such biomimetic particles could prove very useful as RBC surrogates in biomechanical studies. Wheeler and coworkers have also used biotin coated microparticles to simulate the behavior of ligand mediated flow through narrow cavities.<sup>[100]</sup> Microparticles formed using microfluidics were constrained to flow through narrow constrictions coated with avidin. It was found that the speed of such particles is reduced compared to a control particle that has no coating. Further, soft and deformable particles exhibited greater reductions in speed than more rigid particles. Gell shell capsules acting as cell surrogates could also be useful in experimental studies to verify computer simulations that have been used to design patterned surfaces for applications such as sorting of cells.<sup>[101]</sup>

### 5.6. Scale-up and Scale-down

A large majority of microfluidic applications tend to be analytical in nature where the amount of precious sample used must be conserved. Volume reduction is therefore generally regarded as a virtue. Synthesis applications are different. While the micrometer-scale construction of microfluidic devices is essential to ensure the adequate size, shape or anisotropy of the particle, massive scale-up is required to generate particle quantities that are useful for practical applications. Most current methods are capable of synthesizing a few thousand particles per second at best which translates into roughly  $0.2 \text{ g h}^{-1}$  using  $50 \mu\text{m}$  as a reference size. This rules out the use of microfluidics for bulk applications like paints and coatings which require materials at throughputs in the range of tons/h. However, in separation applications for biotechnology where sample volumes tend to be far smaller (in the ml range), quantities in the range of hundreds to thousands of grams per hour of microparticles may be sufficient for commercial purposes. Currently, monodisperse spherical particles that are available for such applications are priced in the range of \$10–100 per gram depending upon the size and chemical moiety conjugated to the particle. The first few steps towards such scale-up for microfluidic reactors have been taken only recently (Fig. 10). Nisisako et al.<sup>[102]</sup> have reported the fabrication of a module that contained a glass chip enclosed in

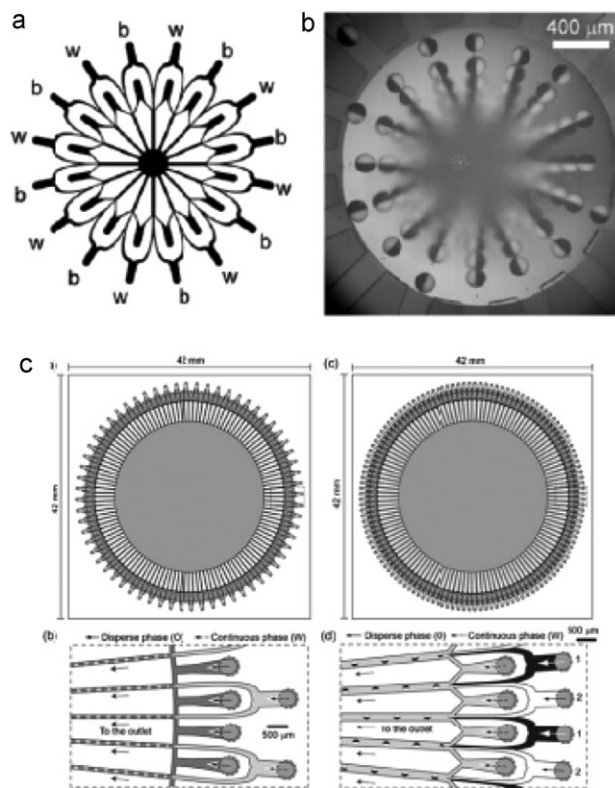


**Figure 10.** Scale-up of microfluidic particle synthesis processes. a) Schematic showing 16 parallel FFDs in a radial configuration. Reproduced with permission from [93]. b) Brightfield microscope image of Janus particle formation at the FFDs shown in a). c) Massively parallelized FFD configuration showing 128 FFDs arranged with circular symmetry. Parallelization schemes for both homogeneous and Janus particles are shown. Reproduced with permission from [102]. Copyright 2008 Royal Society of Chemistry.

a holder for the fabrication of up to 300 grams per hour of acrylic particles. The device could also be used for the synthesis of Janus particles and CVs around 3% or less.

A first step in the scale-up of the flow lithography techniques developed has been addressed with the development of SFL. The next step to increase throughput will be to use wider area collimated lamps to synthesize particles. For instance, using commercially available 6" lamps one can easily synthesize on the order of  $10^{11}$ ,  $3 \mu\text{m}$  particles per second which corresponds to approximately 200 grams per hour. A practical issue of importance here is the sagging of PDMS devices. Channels containing posts at appropriate intervals must be used to make the large devices that will be required. Nisisako and coworkers have taken the lead in commercializing some of the particle technologies developed by them. Soken Chemical & Engineering Company<sup>[103]</sup> in Japan is now in the process of commercializing twisting-ball displays (a kind of e-paper) using the Janus particles produced by microfluidic processing.

For self-assembly by thermal forces, colloidal sized particles with a maximum length scale of a few micrometers are required. For drug delivery applications sub-micrometer-sized particles are preferred. Currently most microfluidic methods are capable of synthesizing particles greater than  $10 \mu\text{m}$  in size (Table 1). This



makes assembly by using only thermal forces impractical. An important challenge, therefore, for microfluidic particle synthesis methods is to adapt to the colloidal length scale while retaining features such as chemical anisotropy.

## 6. Outlook

Microfluidic technologies for the synthesis of particles are still in their infancy. The most exciting results in this field are coming from groups that exploit the unique processing conditions at the micro-scale to produce particles with unprecedented geometric and chemical complexity. This complexity can then be leveraged to develop new applications. The focus in the field must therefore gradually shift from describing particle morphology to describing the end results that will be enabled by the introduction of specific physical characteristics in a particle. The publication of validation and benchmarking studies that compare particle enabled technologies with conventional ones will help microfluidic technologies gain credence among industrial users. Focusing on some of the key advantages that microfluidics confers – customized shapes, high monodispersity and multiple functionality – is certain to yield exciting new applications in the coming years. As in other fields, product based patents which describe the characteristics of the particles synthesized and their usefulness will be more valuable than process based patents which describe the procedure to perform a synthesis. Establishing a link between physical characteristics of the particle and its likely use will make for strong patent claims. It is also likely that microfluidic methods will occupy or create their own space while co-existing with commercially successful and proven technologies like suspension and emulsion polymerization. Drivers in the future for synthesis technologies will come from existing or to be developed applications, fundamental studies of collective and/or motile particle behavior, and pure scientific curiosity. While initial inroads have been made, more work in the area of scale-up must be done.

## Acknowledgements

We gratefully acknowledge the support of NSF NIRT grant no. CTS-0304128 and the Singapore-MIT Alliance (SMA-II, CPE Program) for this project.

Received: November 17, 2008

Revised: March 18, 2009

Published online:

- [1] K. Takamura, D. Urban, *Polymeric Dispersions and Their Industrial Applications*, Wiley-VCH, Weinheim **2002**.
- [2] S. Derveaux, B. G. Stubbe, K. Braeckmans, C. Roelant, K. Sato, J. Demeester, S. C. De Smedt, *Anal. Bioanal. Chem.* **2008**, *391*, 2453.
- [3] S. H. Kim, S. J. Jeon, S. M. Yang, *J. Am. Chem. Soc.* **2008**, *130*, 6040.
- [4] S. C. Glotzer, M. J. Solomon, *Nat. Mater.* **2007**, *6*, 557.
- [5] J. A. Champion, Y. K. Katare, S. Mitragotri, *J. Controlled Release* **2007**, *121*, 3.
- [6] J. P. Rolland, B. W. Maynor, L. E. Euliss, A. E. Exner, G. M. Denison, J. M. DeSimone, *J. Am. Chem. Soc.* **2005**, *127*, 10096.
- [7] J. A. Champion, Y. K. Katare, S. Mitragotri, *Proc. Natl. Acad. Sci. USA* **2007**, *104*, 11901.
- [8] C. J. Hernandez, T. G. Mason, *J. Phys. Chem. C* **2007**, *111*, 4477.
- [9] J. R. Friend, L. Y. Yeo, D. R. Arifin, A. Mechler, *Nanotechnology* **2008**, *19*, 145301.
- [10] S. A. Khan, A. Gunther, M. A. Schmidt, K. F. Jensen, *Langmuir* **2004**, *20*, 8604.
- [11] S. W. Li, H. H. Xu, Y. J. Wang, G. S. Luo, *Langmuir* **2008**, *24*, 4194.
- [12] J. H. Yujun Song, Challa S. S. R. Kumar, *Small* **2008**, *4*, 698.
- [13] B. Laulicht, P. Cheifetz, E. Mathiowitz, A. Tripathi, *Langmuir* **2008**, *24*, 9717.
- [14] W. Engl, R. Backov, P. Panizza, *Curr. Opin. Colloid Interface Sci.* **2008**, *13*, 206.
- [15] C. A. Serra, Z. Q. Chang, *Chem. Eng. Technol.* **2008**, *31*, 1099.
- [16] J. L. Steinbacher, D. T. McQuade, *J. Polym. Sci. Part A* **2006**, *44*, 6505.
- [17] G. F. Christopher, S. L. Anna, *J. Phys. D* **2007**, *40*, R319.
- [18] T. Kawakatsu, Y. Kikuchi, M. Nakajima, *J. Am. Oil Chem. Soc.* **1997**, *74*, 317.
- [19] T. Thorsen, R. W. Roberts, F. H. Arnold, S. R. Quake, *Phys. Rev. Lett.* **2001**, *86*, 4163.
- [20] P. Garstecki, M. J. Fuerstman, H. A. Stone, G. M. Whitesides, *Lab Chip* **2006**, *6*, 437.
- [21] A. Kubo, H. Shinmori, T. Takeuchi, *Chem. Lett.* **2006**, 588.
- [22] M. L. J. Steegmans, K. G. P. H. Schroelín, R. M. Boom, *Langmuir* **2009**, *25*, 3396.
- [23] S. L. Anna, N. Bontoux, H. A. Stone, *Appl. Phys. Lett.* **2003**, *82*, 364.
- [24] A. M. Ganan-Calvo, *Phys. Rev. Lett.* **1998**, *80*, 285.
- [25] W. J. Jeong, J. Y. Kim, J. Choo, E. K. Lee, C. S. Han, D. J. Beebe, G. H. Seong, S. H. Lee, *Langmuir* **2005**, *21*, 3738.
- [26] A. S. Utada, A. Fernandez-Nieves, H. A. Stone, D. A. Weitz, *Phys. Rev. Lett.* **2007**, *99*, 094502.
- [27] E. Quevedo, J. Steinbacher, D. T. McQuade, *J. Am. Chem. Soc.* **2005**, *127*, 10498.
- [28] A. S. Utada, E. Lorenceau, D. R. Link, P. D. Kaplan, H. A. Stone, D. A. Weitz, *Science* **2005**, *308*, 537.
- [29] S. Sugiura, M. Nakajima, J. H. Tong, H. Nabetani, M. Seki, *J. Colloid Interface Sci.* **2000**, *227*, 95.
- [30] S. Sugiura, M. Nakajima, H. Itou, M. Seki, *Macromol. Rapid Commun.* **2001**, *22*, 773.
- [31] S. Sugiura, T. Oda, Y. Izumida, Y. Aoyagi, M. Satake, A. Ochiai, N. Ohkohchi, M. Nakajima, *Biomaterials* **2005**, *26*, 3327.
- [32] W.-H. Tan, S. Takevchi, *Adv. Mater.* **2007**, *19*, 2696.
- [33] T. Nisisako, T. Torii, T. Higuchi, *Chem. Eng. J.* **2004**, *101*, 23.
- [34] D. Dendukuri, K. Tsoi, T. A. Hatton, P. S. Doyle, *Langmuir* **2005**, *21*, 2113.
- [35] S. Xu, Z. Nie, M. Seo, P. Lewis, E. Kumacheva, H. A. Stone, P. Garstecki, D. B. Weibel, I. Gitlin, G. M. Whitesides, *Angew. Chem. Int. Ed.* **2005**, *44*, 724.
- [36] M. Seo, Z. Nie, S. Xu, P. C. Lewis, E. Kumacheva, *Langmuir* **2005**, *21*, 4773.
- [37] Z. Nie, S. Xu, M. Seo, P. C. Lewis, E. Kumacheva, *J. Am. Chem. Soc.* **2005**, *127*, 8058.
- [38] T. Nisisako, T. Torii, *Adv. Mater.* **2007**, *19*, 1489.
- [39] S. L. Anna, H. C. Mayer, *Phys. Fluids* **2006**, *18*.
- [40] P. J. A. Kenis, R. F. Ismagilov, G. M. Whitesides, *Science* **1999**, *285*, 83.
- [41] P. G. de Gennes, *Rev. Mod. Phys.* **1992**, *64*, 645.
- [42] A. Walther, A. H. E. Muller, *Soft Matter* **2008**, *4*, 663.
- [43] Z. H. Nie, W. Li, M. Seo, S. Q. Xu, E. Kumacheva, *J. Am. Chem. Soc.* **2006**, *128*, 9408.
- [44] G. A. Gross, C. Hamann, M. Gunther, J. M. Kohler, *Chem. Eng. Technol.* **2007**, *30*, 341.
- [45] D. K. Hwang, D. Dendukuri, P. S. Doyle, *Lab Chip* **2008**, *8*, 1640.
- [46] R. F. Shepherd, J. C. Conrad, S. K. Rhodes, D. R. Link, M. Marquez, D. A. Weitz, J. A. Lewis, *Langmuir* **2006**, *22*, 8618.
- [47] T. Nisisako, *Chem. Eng. Technol.* **2008**, *31*, 1091.
- [48] S. Okushima, T. Nisisako, T. Torii, T. Higuchi, *Langmuir* **2004**, *20*, 9905.
- [49] V. Barbier, M. Tatoulian, H. Li, F. Arefi-Khonsari, A. Ajdari, P. Tabeling, *Langmuir* **2006**, *22*, 5230.

- [50] J. W. Kim, A. S. Utada, A. Fernandez-Nieves, Z. Hu, D. A. Weitz, *Angew. Chem. Int. Ed.* **2007**, *46*, 1819.
- [51] A. B. Jiandi Wan, M. Sullivan, H. A. Stone, *Adv. Mater.* **2008**, *20*, 3314.
- [52] S. L. Peng, M. Y. Zhang, X. Z. Niu, W. J. Wen, P. Sheng, Z. Y. Liu, J. Shi, *Appl. Phys. Lett.* **2008**, *92*.
- [53] S. Dubinsky, H. Zhang, Z. H. Nie, I. Gourevich, D. Voicu, M. Deetz, E. Kumacheva, *Macromolecules* **2008**, *41*, 3555.
- [54] D. Dendukuri, D. C. Pregonon, J. Collins, T. A. Hatton, P. S. Doyle, *Nat. Mater.* **2006**, *5*, 365.
- [55] D. Dendukuri, S. S. Gu, D. C. Pregonon, T. A. Hatton, P. S. Doyle, *Lab Chip* **2007**, *7*, 818.
- [56] J. C. Love, D. B. Wolfe, H. O. Jacobs, G. M. Whitesides, *Langmuir* **2001**, *17*, 6005.
- [57] C. Decker, A. D. Jenkins, *Macromolecules* **1985**, *18*, 1241.
- [58] D. Dendukuri, P. Panda, R. Haghgoie, J. M. Kim, T. A. Hatton, P. S. Doyle, *Macromolecules* **2008**, *41*, 8547.
- [59] W. Jeong, J. Kim, S. Kim, S. Lee, G. Mensing, D. J. Beebe, *Lab Chip* **2004**, *4*, 576.
- [60] D. J. Beebe, J. S. Moore, J. M. Bauer, Q. Yu, R. H. Liu, C. Devadoss, B.-H. Jo, *Nature* **2000**, *404*, 588.
- [61] J. H. Jang, D. Dendukuri, T. A. Hatton, E. L. Thomas, P. S. Doyle, *Angew. Chem. Int. Ed.* **2007**, *46*, 9027.
- [62] K. W. Bong, D. C. Pregonon, P. S. Doyle, *Lab Chip* **2009**, *9*, 863.
- [63] S. A. Lee, S. E. Chung, W. Park, S. H. Lee, S. Kwon, *Lab Chip* **2009**, DOI:10.1039/b819999j.
- [64] P. S. Doyle, D. C. Pregonon, D. Dendukuri, *US Patent Application Number PCT/US2006/041668*, **2007**.
- [65] S. E. Chung, W. Park, H. Park, K. Yu, N. Park, S. Kwon, *Appl. Phys. Lett.* **2007**, *91*, 041106.
- [66] P. Panda, K. P. Yuet, T. A. Hatton, P. S. Doyle, *Langmuir* DOI:10.1021/1a80424445.
- [67] S. E. Chung, W. Park, S. Shin, S. A. Lee, S. Kwon, *Nat. Mater.* **2008**, *7*, 581.
- [68] D. C. Pregonon, M. Toner, P. S. Doyle, *Science* **2007**, *315*, 1393.
- [69] D. Dendukuri, T. A. Hatton, P. S. Doyle, *Langmuir* **2007**, *23*, 4669.
- [70] R. F. Shepherd, P. Panda, Z. Bao, K. H. Sandhage, T. A. Hatton, J. A. Lewis, P. S. Doyle, *Adv. Mater.* **2008**, *20*, 4734.
- [71] W. S. Tan, C. L. Lewis, N. E. Horelik, D. C. Pregonon, P. S. Doyle, H. Yi, *Langmuir* **2008**, *24*, 12483.
- [72] E. M. Furst, C. Suzuki, M. Fermigier, A. P. Gast, *Langmuir* **1998**, *14*, 7334.
- [73] H. Singh, P. E. Laibinis, T. A. Hatton, *Langmuir* **2005**, *21*, 11500.
- [74] H. Singh, P. E. Laibinis, T. A. Hatton, *Nano Lett.* **2005**, *5*, 2149.
- [75] O. D. Velev, A. M. Lenhoff, E. W. Kaler, *Science* **2000**, *287*, 2240.
- [76] J. R. Millman, K. H. Bhatt, B. G. Prevo, O. D. Velev, *Nat. Mater.* **2005**, *4*, 98.
- [77] V. N. Manoharan, M. T. Elsesser, D. J. Pine, *Science* **2003**, *301*, 483.
- [78] V. N. Manoharan, A. Imhof, J. D. Thorne, D. J. Pine, *Adv. Mater.* **2001**, *13*, 447.
- [79] G. R. Yi, S. J. Jeon, T. Thorsen, V. N. Manoharan, S. R. Quake, D. J. Pine, S. M. Yang, *Synth. Met.* **2003**, *139*, 803.
- [80] G. R. Yi, T. Thorsen, V. N. Manoharan, M. J. Hwang, S. J. Jeon, D. J. Pine, S. R. Quake, S. M. Yang, *Adv. Mater.* **2003**, *15*, 1300.
- [81] Y. D. Yin, Y. N. Xia, *J. Am. Chem. Soc.* **2003**, *125*, 2048.
- [82] Y. Xia, Y. Yin, Y. Lu, J. McLellan, *Adv. Funct. Mater.* **2003**, *13*, 907.
- [83] Y. D. Yin, Y. Lu, B. Gates, Y. N. Xia, *J. Am. Chem. Soc.* **2001**, *123*, 8718.
- [84] K. E. Sung, S. A. Vanapalli, D. Mukhija, H. A. McKay, J. M. Millunchick, M. A. Burns, M. J. Solomon, *J. Am. Chem. Soc.* **2008**, *130*, 1335.
- [85] A. B. Subramaniam, M. Abkarian, L. Mahadevan, H. A. Stone, *Nature* **2005**, *438*, 930.
- [86] A. B. Subramaniam, M. Abkarian, H. A. Stone, *Nat. Mater.* **2005**, *4*, 553.
- [87] O. Lehmann, M. Stuke, *Science* **1995**, *270*, 1644.
- [88] R. Attia, D. C. Pregonon, P. S. Doyle, J.-L. Viovy, D. Bartolo, *Lab Chip* **2009**, *9*, 1213.
- [89] K. Haupt, *Analyst* **2001**, *126*, 747.
- [90] M. Zourob, S. Mohr, A. G. Mayes, A. Macaskill, N. Perez-Moral, P. R. Fielden, N. J. Goddard, *Lab Chip* **2006**, *6*, 296.
- [91] S.-H. Kim, S.-J. Jeon, G.-R. Yi, C.-J. Heo, J. H. Choi, S.-M. Yang, *Adv. Mater.* **2008**, *20*, 1649.
- [92] C. Goubault, P. Jop, M. Fermigier, J. Baudry, E. Bertrand, J. Bibette, *Phys. Rev. Lett.* **2003**, *91*, 260802.
- [93] T. Nisisako, T. Torii, T. Takahashi, Y. Takizawa, *Adv. Mater.* **2006**, *18*, 1152.
- [94] S. Sugiura, T. Oda, Y. Aoyagi, R. Matsuo, T. Enomoto, K. Matsumoto, T. Nakamura, M. Satake, A. Ochiai, N. Ohkohchi, M. Nakajima, *Biomed. Microdevices* **2007**, *9*, 91.
- [95] P. Panda, S. Ali, E. Lo, B. G. Chung, T. A. Hatton, A. Khademhosseini, P. S. Doyle, *Lab Chip* **2008**, *8*, 1056.
- [96] S. Freitas, H. P. Merkle, B. Gander, *J. Controlled Release* **2005**, *102*, 313.
- [97] C. Wischke, D. Lorenzen, J. Zimmermann, H.-H. Borchert, *Eur. J. Pharm. Biopharm.* **2006**, *62*, 247.
- [98] S. Freitas, A. Walz, H. P. Merkle, B. Gander, *J. Microencapsulation* **2003**, *20*, 67.
- [99] R. Haghgoie, P. S. Doyle, *Proceedings of  $\mu$ TAS*, San Diego, **2008**.
- [100] L. K. Fiddes, K. W. H. K. C. Chan, C. A. Simmons, E. Kumacheva, A. R. Wheeler, *Lab Chip* **2009**, *9*, 286.
- [101] O. B. Usta, M. Nayhouse, A. Alexeev, A. C. Balazs, *J. Chem. Phys.* **2008**, *128*, 235102.
- [102] T. Nisisako, T. Torii, *Lab Chip* **2008**, *8*, 287.
- [103] <http://www.soken-ce.co.jp/english/index.html> (accessed on May 8, 2009).
- [104] T. Nisisako, S. Okushima, T. Torii, *Soft Matter* **2005**, *1*, 23.
- [105] S. A. Vanapalli, C. R. Iacovella, K. E. Sung, D. Mukhija, J. M. Millunchick, M. A. Burns, S. C. Glotzer, M. J. Solomon, *Langmuir* **2008**, *24*, 3661.
- [106] S. F. Kingsmore, *Nat. Rev. Drug Discovery* **2006**, *5*, 310.
- [107] H. Zhang, E. Tumarkin, R. Peerani, Z. Nie, R. M. A. Sullan, G. C. Walker, E. Kumacheva, *J. Am. Chem. Soc.* **2006**, *128*, 12205.
- [108] S. Iwamoto, K. Nakagawa, S. Sugiura, M. Nakajima, *AAPS PharmSciTech* **2002**, *3*, E25.
- [109] B. G. De Geest, J. P. Urbanski, T. Thorsen, J. Demeester, S. C. De Smedt, *Langmuir* **2005**, *21*, 10275.
- [110] X. Gong, S. Peng, W. Wen, P. Sheng, W. Li, *Adv. Funct. Mater.* **2009**, *19*, 292.
- [111] J. L. Steinbacher, R. W. Y. Moy, K. E. Price, M. A. Cummings, C. Roychowdhury, J. J. Buffy, W. L. Olbricht, M. Haaf, D. T. McQuade, *J. Am. Chem. Soc.* **2006**, *128*, 9442.
- [112] S. Abraham, Y. H. Park, J. K. Lee, C. S. Ha, I. Kim, *Adv. Mater.* **2008**, *20*, 2177.
- [113] C.-H. Chen, R. K. Shah, A. R. Abate, D. A. Weitz, *Langmuir* **2009**, *25*, 4320.
- [114] D. K. Hwang, J. Oakey, M. Toner, J. A. Arthur, K. S. Anseth, S. Lee, A. Zeiger, K. J. Van Vliet, P. S. Doyle, *J. Am. Chem. Soc.* **2009**, *131*, 4499.
- [115] Q. Y. Xu, M. Nakajima, B. P. Binks, *Colloids Surf. A* **2005**, *262*, 94.